

Dye-Sensitized Solar Cells

Ruthenium(II) Sensitizers with Heteroleptic Tridentate Chelates for Dye-Sensitized Solar Cells**

Chun-Cheng Chou, Kuan-Lin Wu, Yun Chi,* Wei-Ping Hu, Shuchun Joyce Yu, Gene-Hsiang Lee, Chia-Li Lin, and Pi-Tai Chou

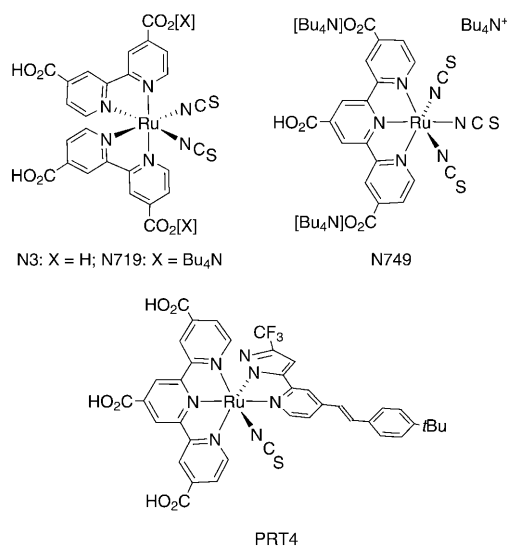
Dye-sensitized solar cells (DSSCs) are a promising technology with the potential to harvest sunlight at low cost.^[1] Specifically, DSSCs based on either organometallic dyes^[2] or organic push-and-pull dyes^[3] adsorbed on nanocrystalline TiO₂ photoanodes have attracted intensive research interest in the past two decades. The use of ruthenium(II)-based sensitizers^[4] is still the most attractive approach, because their photophysical and electrochemical properties can be systematically fine-tuned to achieve optimal material characteristics. Key examples of Ru^{II} sensitizers for DSSCs include the well-established N3 and N719 dyes and their functionalized derivatives.^[5,6] These dyes are commonly assembled by incorporation of at least one 4,4'-dicarboxy-2,2'-bipyridine chelate (Scheme 1), on which the carboxy anchors allow

efficient electron injection into the TiO₂ nanoparticles. The accompanying thiocyanate ancillary ligands are pointed away from the TiO₂ surface, thus providing intimate contact to the I⁻/I₃⁻ redox couple in the electrolyte and subsequently triggering rapid regeneration of the oxidized sensitizer. The lower-lying absorption bands are attributed to metal-to-ligand charge transfer (MLCT) and display absorption thresholds close to 800 nm, unmatched by the majority of organic dyes known to date.

For optimizing Ru^{II} sensitizers, it has been reported that, upon introduction of 4,4',4''-tricarboxy-2,2':6,2''-terpyridine (H₃tctpy), the lowest energy transition could be extended toward the near-IR region, thus affording the panchromatic sensitizer known as N749, or black dye [nBu₄N]₃[Ru(Htctpy)-(NCS)₃].^[7] Although this design seems to show satisfactory sensitization up to 900 nm, it still possesses two major deficiencies. One is the inferior absorptivity in the visible region, attributed to the lack of effective auxochrome. The second is the presence of three thiocyanate ligands, which not only reduce the synthetic yield owing to coordination isomerism^[7,8] but also deteriorate the lifespan of the as-fabricated cell units, because the weak Ru–NCS dative bonding causes notable dye decomposition during operation.

In conjunction with current endeavors, we described one panchromatic dye PRT4, which possesses a styrene-substituted pyridyl pyrazolate (pypz) auxochrome.^[9] Its recorded solar-cell performance supersedes our best reference cells using N749, thus providing the first success for our research initiative. Herein we present a breakthrough design employing both the H₃tctpy anchor and a newly designed tridentate ancillary ligand; the latter is also targeted for replacing the last remaining thiocyanate in our PRT4 dye as well as all three thiocyanates in N749 sensitizer. Thiophene derivatives or other auxochrome units were tethered to the central pyridyl group in an attempt to increase the light-harvesting capability.

In this synthetic protocol (Scheme 2), the functionalized 2,6-bis(5-pyrazolyl)pyridine chelate was first prepared using a multistep process starting from chlorination of chelidamic acid,^[10] except for the synthesis of parent 2,6-bis(5-pyrazolyl)pyridine, which employed the commercially available 2,6-diacetylpyridine. Bis-tridentate Ru^{II} complexes were then obtained from addition of the relevant 2,6-dipyrazolylpyridine derivative with source complex [Ru(tectpy)Cl₃] in ethanol solution (tectpy = 4,4',4''-triethoxycarbonyl-2,2':6',2''-terpyridine). The crude ethoxycarbonyl Ru^{II} products were purified on a silica gel column and eluted with a mixture of hexane and ethyl acetate. To confirm their molecular structure, single-crystal X-ray analysis of one derivative (TF-2OEt; TF = thiocyanate-free) was carried



Scheme 1. Ru^{II} sensitizers N3, N719, N749, and PRT4.

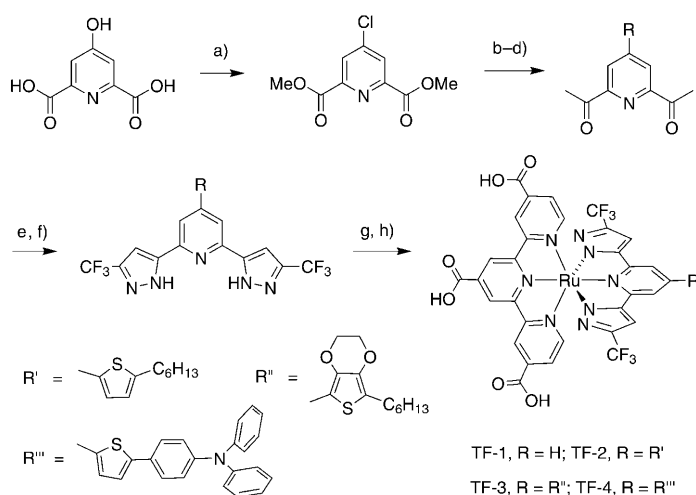
[*] C.-C. Chou, K.-L. Wu, Prof. Y. Chi
Department of Chemistry, National Tsing Hua University
Hsinchu, Taiwan 30013 (Taiwan)
E-mail: ychi@mx.nthu.edu.tw

Prof. W.-P. Hu, Prof. S. J. Yu
Department of Chemistry and Biochemistry
National Chung Cheng University (Taiwan)

Dr. G.-H. Lee, C.-L. Lin, Prof. P.-T. Chou
Department of Chemistry
National Taiwan University (Taiwan)

[**] This research was supported by the National Science Council (NSC-98-3114-E-007-005)

Supporting information for this article is available on the WWW under <http://dx.doi.org/10.1002/anie.201006629>.



Scheme 2. Synthetic route to the Ru^{II} sensitizers TF-1–TF-4. Reagents and conditions: a) PCl₅, CHCl₃, MeOH; b) EtOAc, NaOEt, reflux; c) HCl_(aq), reflux; d) Suzuki or Stille coupling, [Pd(PPh₃)₄]; e) CF₃CO₂Et, NaOEt, THF, reflux; f) N₂H₄, EtOH, reflux; g) [Ru(tectpy)Cl₃], EtOH, reflux; h) NaOH, acetone/H₂O, acidification.

out (see Figure S1 in the Supporting Information for the ORTEP diagram and the associated metric parameters). Then hydrolysis of ethoxycarbonyl groups was conducted in a basified acetone/water mixture, and the Ru^{II} sensitizers were precipitated from the solution by adjusting the pH value to 3. To improve purity, these precipitates were then crystallized by slow diffusion of diethyl ether into a saturated DMF solution at room temperature. The identity of all sensitizers TF-1–TF-4 was verified by routine mass spectrometry, ¹H NMR spectroscopy, and elemental analysis. Owing to the dual tridentate nature of the complex, the sole product was obtained free from 1) the interference of thiocyanate isomerism and 2) the otherwise mandatory H⁺/Bu₄N⁺ metathesis. Accordingly, the yield of isolated product was increased to 67% starting from [Ru(tectpy)Cl₃] (cf. 46% for N749).^[7]

The absorption spectra of our TF dyes in DMF solution are depicted in Figure 1 together with that of N749 for

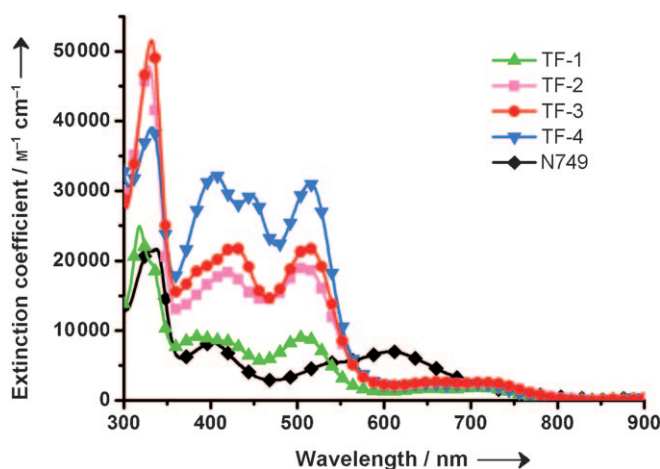


Figure 1. Absorption spectra of TF-1–TF-4 and N749 in DMF.

comparison. Their pertinent photophysical and electrochemical properties are summarized in Table 1. These TF dyes show intense visible absorption bands down to 510 nm, which are assigned to metal-to-ligand charge transfer (MLCT) to the H₃tctpy chelate, together with contributions from ligand-to-ligand charge transfer (LLCT) originating from the pyrazolate groups. A further difference from N749 is that all TF dyes exhibit broad absorption at the longer-wavelength region, with two weak peak maxima centered at about 650 and 720 nm and with a shoulder extending to 800 nm; these features are attributed to a mixed MLCT and LLCT transition (to H₃tctpy). Notably, the intense MLCT band at 606 nm in N749 is substantially suppressed in all TF dyes, which could be due to the lack of the three thiocyanate anions. This spectral assignment is further supported by theoretical calculations (see details in the Supporting Information). Using TF-2 as an example, Figure 2 depicts selected optically active electronic transitions (black bars) employing time-dependent (TD) DFT PCM calculations in DMF as media. According to the calculations, the

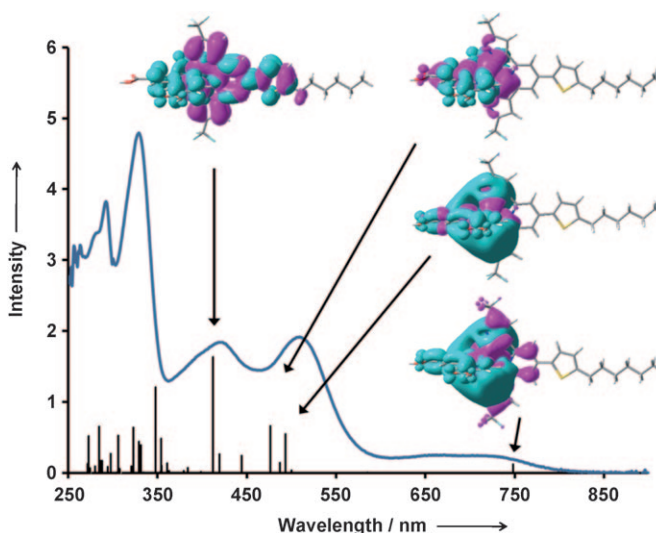


Figure 2. Experimental absorption spectrum of TF-2 sensitizer in DMF and the associated calculated spectrum. Black bars represent the computed vertical electronic excitations intensities (*f*) by TD-DFT method. The electron–hole density plots are shown for the selected electronic transitions at 412, 476, 493, and 748 nm, for which hole and excited electron densities are represented in pink and cyan, respectively.

absorption bands in the higher-energy region of 410–450 nm are ascribed to S₁₁–S₁₅ excitation, for which the frontier orbital analyses indicate that electron density, in part, is distributed around the thiophene moiety (see electron–hole density at 412 nm, Figure 2).

Cyclic voltammetry was conducted to ensure that the highest occupied molecular orbitals (HOMOs) of all TF sensitizers match the redox potential of electrolyte and to verify whether their lowest unoccupied molecular orbitals (LUMOs) are higher than the conduction band of TiO₂. As shown in Table 1, the onset potential for Ru^{II} metal oxidation

Table 1: Photophysical and electrochemical data of TF-1 to TF-4 measured in DMF. Also included are the respective photovoltaic parameters under global AM 1.5 irradiation for DSSCs adsorbed on nanocrystalline TiO₂ anodes.

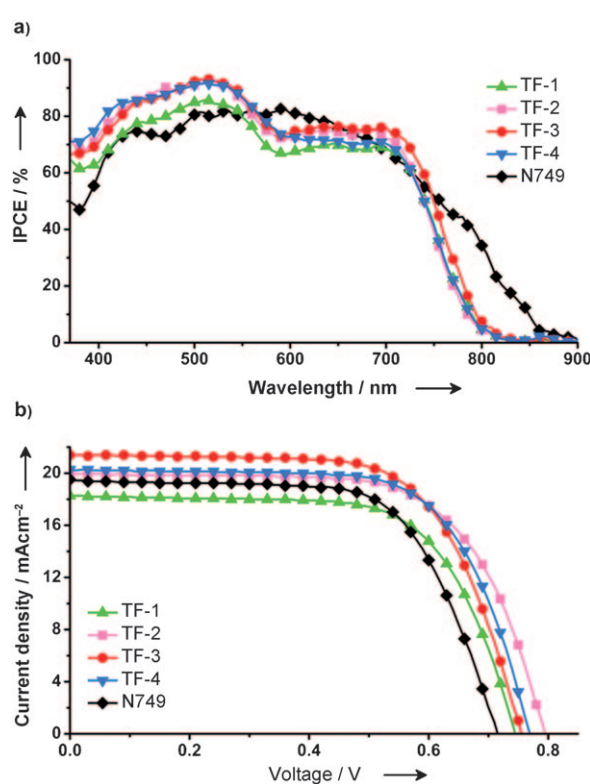
Dye	λ_{abs} [nm] (ϵ [L mol ⁻¹ cm ⁻¹]) ^[a]	λ_{em} [nm] ^[a]	E°_{ox} [V] ^[b]	E_{0-0} [V] ^[c]	E_{LUMO} [V] ^[d]	V_{OC} [V]	J_{SC} [mA cm ⁻²]	FF	η [%] ^[e]
TF-1	318 (24906), 383 (9123), 417 (8507), 510 (9067), 640 (1623), 721 (1735)	772, 830 (sh)	0.94	1.70	-0.76	740	18.22	0.676	9.11
TF-2	329 (47898), 421 (18396), 509 (19170), 654 (2541), 719 (2430)	770, 827 (sh)	0.95	1.68	-0.73	790	20.00	0.665	10.5
TF-3	322 (51599), 387 (18763), 426 (21956), 513 (21890), 653 (2671), 723 (2606)	760, 825 (sh)	0.97	1.72	-0.75	760	21.39	0.660	10.7
TF-4	333(39037), 404(32366), 447 (29334), 516 (30926), 662 (2349), 716 (2350)	770, 826 (sh)	0.94	1.69	-0.75	770	20.27	0.675	10.5
N749	400 (8219), 606 (7003)	–	–	–	–	720	19.49	0.657	9.22

[a] Photophysical data were measured in DMF; sh = shoulder. [b] Oxidation potential of dyes was measured in DMF with 0.1 M (nBu)₄NPF₆ and with a scan rate of 50 mV s⁻¹ (vs. the normal hydrogen electrode, NHE). It was calibrated with ferrocene/ferrocenium as internal reference and converted to NHE by addition of 0.63 V. [c] E_{0-0} (the difference in zero-point energy between the S₀ and T₁ states) was determined from the average of absorption (lowest-lying peak) and emission peak in terms of energy (eV) in DMF. [d] E_{LUMO} was calculated according to the equation $E_{\text{ox}} - E_{0-0}$. [e] All devices were fabricated using a 15 μm layer of TiO₂ nanoparticles (20 nm) and a 5 μm layer of 400 nm scattering particles (TiO₂), while performance characteristics were measured with a 0.144 cm² working area.

appeared in the range 0.94–0.97 V (vs. NHE), showing that the I⁻/I₃⁻ redox couple (ca. 0.4 V vs. NHE) is more negative than the respective HOMOs and is able to regenerate the dye efficiently. The LUMO energy levels, estimated from the difference of the HOMO and the onset of the optical energy gap (see Table 1), are also sufficiently more negative than the conduction band edge of the TiO₂ electrode (ca. -0.5 V vs. NHE).

The DSSC performance of these sensitizers was then examined using a 15 μm thick layer of 20 nm TiO₂ nanoparticles plus a 5 μm thick layer of 400 nm scattering particles (TiO₂) with an acetonitrile electrolyte containing 0.6 M 1,2-dimethyl-3-propylimidazolium iodide, 0.1 M iodine, 0.5 M *tert*-butylpyridine, and 0.1 M lithium iodide. The incident photon-to-current conversion efficiencies (IPCEs) of these DSSC dyes are shown in Figure 3 a. The onsets of the IPCE spectra are all close to 820 nm, and excellent IPCE performance was observed from 420 to 700 nm. It is notable that, except for the parent TF-1, which exhibits a maximum IPCE of 85% at 515 nm, all other sensitizers (TF-2–TF-4) show a much better IPCE value of 92% at 515 nm and maintain a high value of approximately 75% in the longer wavelength region up to 685 nm. For comparison, DSSC fabricated using N749 showed inferior IPCE below 560 nm and in the region between 640 and 710 nm and increased IPCE in the regions between 560 and 640 nm and beyond 730 nm.

Figure 3 b shows the photocurrent density–voltage curve of the DSSC devices recorded under AM 1.5 G simulated sunlight at a light intensity of 100 mW cm⁻². The N749 cells showed short-circuit current density (J_{SC}), open-circuit voltage (V_{OC}), fill factor (FF), and overall conversion efficiency (η) of 19.49 mA cm⁻², 720 mV, 0.657, and 9.22%, respectively. We note, however, that this conversion efficiency is lower than that reported by Wang et al. (10.5%) and by Han et al. (11.1%).^[11,12] Remarkably, most of our TF-sensitized solar cells were endowed with much better, double-digit efficiencies. For instance, TF-3 gives $J_{\text{SC}} = 21.39$ mA cm⁻², $V_{\text{OC}} = 760$ mV, and $FF = 0.66$, corresponding to an overall conversion efficiency $\eta = 10.7\%$. The higher V_{OC} seems unrelated to the neutral characteristics of the TF sensitizers. If this were


Figure 3. a) Photon-to-current action spectra and b) current–voltage characteristics of solar cells sensitized with various TF dyes and N749.

the case, N749 would be expected to have an even higher V_{OC} , because it carries only one proton, while the investigated TF sensitizers carry three protons. For comparison, a reduction of the number of protons in either N3 or N719 was found to induce an increase of V_{OC} as large as 90 mV.^[13] Alternatively, we propose that the replacement of the three thiocyanate ligands with the extremely bulky 2,6-bis(5-pyrazolyl)pyridine ligand may allow better packing upon adsorption on the TiO₂ surface, which could prevent interfacial charge recombination,^[14] thus giving the first advantage. Moreover, in compar-

ison to the prevailing negative contribution of the thiocyanate ligands that reside at the similar site of N749, the neutral pyridyl group flanked by two 2,6-bis(5-pyrazolyl) termini may be intrinsically more capable of exerting a dipole moment pointing toward the TiO₂ surface.^[15] In other words, in TF sensitizers the negative pole of the dipole moment is expected to localize much closer to the TiO₂ surface, thus giving better lifting of conduction-band energy level and consequently affording higher V_{OC} .^[16] Finally, all functionalized sensitizers (TF-2 to TF-4) show higher current density of 20.00–21.39 mA cm⁻² versus that of 19.49 mA cm⁻² for N749 and 18.22 mA cm⁻² for the parent TF-1, manifesting the increase of molar absorptivity upon extending the π conjugation of the auxochrome.

To gain more insight into the cell characteristics, alternating current (AC) electrochemical impedance spectroscopy was performed to analyze the effects on charge generation, transport, and collection. Figure S2a in the Supporting Information depicts the impedance spectra of DSSCs fabricated with all TF cells in the dark under forward bias (−0.74 V). As a result, the radius of these semicircles reveals a descending order of TF-2 (148.15 Ω) > TF-4 (117.55 Ω) > TF-3 (101.39 Ω) > TF-1 (74.63 Ω) > N749 (65.8 Ω), thus indicating that the recombination process from the as-prepared TF dye-sensitized solar cells is slower than with N749, leading to the higher photovoltage. Concomitantly, the AC electrochemical impedance of the cells was also measured under solar illumination at 1 sun (100 mW cm⁻²). As can be seen in Figure S2b in the Supporting Information, the radius of the semicircle in the intermediate frequency regime, according to the Nyquist plot, follows the opposite order (cf. Figure S2a measured in the dark) of TF-2 < TF-4 < TF-3 < TF-1 < N749. These results clearly indicate that the charge transport is in the order of TF-2 > TF-4 > TF-3 > TF-1 > N749, which coincides with the overall device performances shown in Table 1.

Finally, the lifespan of solar cells fabricated with TF-2 on a (8 + 5) μ m thick TiO₂ photoanode was examined using a long-term accelerated aging experiment under accelerated visible-light soaking at 60 °C. After 1000 h illumination, the device efficiency changed only slightly for all the parameters: J_{SC} 15.73 to 15.95 mA cm⁻², V_{OC} 760 to 690 mV, FF 0.673 to 0.688, and η 8.07 to 7.57% (see Figure S3 in the Supporting Information), thus supporting the advantage of thiocyanate-free, charge-neutral Ru^{II} sensitizers suited for dye-sensitized solar cells.

In summary, promising device performance data have been obtained with the new design of panchromatic Ru^{II} sensitizers that incorporate both 4,4',4''-tricarboxy-2,2':6,2''-terpyridine and 2,6-bis(5-pyrazolyl)pyridine ligands; the best cell showed power conversion efficiencies as high as 10.7%. This result completely rules out the need for thiocyanate ancillary ligands. From a synthetic point of view, the dual tridentate structure avoids problematic isomerization, thus simplifying the purification process and rendering good product yield. Chemically, the multidentate coordination, in theory, should improve the long-term stability, as evidenced by the great lifespan of solar cells fabricated with TF-2. Further development is versatile. Particularly, our strategy even simplifies the structural design that may allow the

negative dipole of sensitizers to reside closer to the TiO₂ surface, which is the prerequisite for raising the TiO₂ conduction-band energy level to achieve high open-circuit voltage (V_{OC}) and decent overall efficiency (η).

Received: October 22, 2010

Published online: January 26, 2011

Keywords: N ligands · pyrazole · ruthenium · sensitizers · thiophene

- [1] a) A. Hagfeldt, G. Boschloo, H. Lindstroem, E. Figgemeier, A. Holmberg, V. Aranyos, E. Magnusson, L. Malmqvist, *Coord. Chem. Rev.* **2004**, *248*, 1501; b) L. M. Gonçalves, V. de Zea Bermudez, H. A. Ribeiro, A. M. Mendes, *Energy Environ. Sci.* **2008**, *1*, 655; c) S. Yanagida, Y. Yu, K. Manseki, *Acc. Chem. Res.* **2009**, *42*, 1827; d) M. Grätzel, *Acc. Chem. Res.* **2009**, *42*, 1788; e) S. Ardo, G. J. Meyer, *Chem. Soc. Rev.* **2009**, *38*, 115; f) Y. Luo, D. Li, Q. Meng, *Adv. Mater.* **2009**, *21*, 4647; g) Z. Ning, Y. Fu, H. Tian, *Energy Environ. Sci.* **2010**, *3*, 1170; h) A. Hagfeldt, G. Boschloo, L. Sun, L. Kloo, H. Pettersson, *Chem. Rev.* **2010**, *110*, 6595.
- [2] a) M. K. Nazeeruddin, C. Klein, P. Liska, M. Grätzel, *Coord. Chem. Rev.* **2005**, *249*, 1460; b) N. Robertson, *Angew. Chem.* **2006**, *118*, 2398; *Angew. Chem. Int. Ed.* **2006**, *45*, 2338; c) H. Imahori, T. Umeyama, S. Ito, *Acc. Chem. Res.* **2009**, *42*, 1809.
- [3] a) Y. Ooyama, Y. Harima, *Eur. J. Org. Chem.* **2009**, 2903; b) Z. Ning, H. Tian, *Chem. Commun.* **2009**, 5483; c) A. Mishra, M. K. R. Fischer, P. Bauerle, *Angew. Chem.* **2009**, *121*, 2510; *Angew. Chem. Int. Ed.* **2009**, *48*, 2474; d) D.-Y. Chen, Y.-Y. Hsu, H.-C. Hsu, B.-S. Chen, Y.-T. Lee, H. Fu, M.-W. Chung, S.-H. Liu, H.-C. Chen, Y. Chi, P.-T. Chou, *Chem. Commun.* **2010**, *46*, 5256.
- [4] a) K.-J. Jiang, N. Masaki, J.-B. Xia, S. Noda, S. Yanagida, *Chem. Commun.* **2006**, 2460; b) C.-Y. Chen, S.-J. Wu, J.-Y. Li, C.-G. Wu, J.-G. Chen, K.-C. Ho, *Adv. Mater.* **2007**, *19*, 3888; c) K.-S. Chen, W.-H. Liu, Y.-H. Wang, C.-H. Lai, P.-T. Chou, G.-H. Lee, K. Chen, H.-Y. Chen, Y. Chi, F.-C. Tung, *Adv. Funct. Mater.* **2007**, *17*, 2964; d) C.-Y. Chen, J.-G. Chen, S.-J. Wu, J.-Y. Li, C.-G. Wu, K.-C. Ho, *Angew. Chem.* **2008**, *120*, 7452; *Angew. Chem. Int. Ed.* **2008**, *47*, 7342; e) F. Gao, Y. Wang, D. Shi, J. Zhang, M. Wang, X. Jing, R. Humphry-Baker, P. Wang, S. M. Zakeeruddin, M. Grätzel, *J. Am. Chem. Soc.* **2008**, *130*, 10720; f) F. Gao, Y. Wang, J. Zhang, D. Shi, M. Wang, R. Humphry-Baker, P. Wang, S. M. Zakeeruddin, M. Grätzel, *Chem. Commun.* **2008**, 2635; g) C. Lee, J.-H. Yum, H. Choi, S. O. Kang, J. Ko, R. Humphry-Baker, M. Grätzel, M. K. Nazeeruddin, *Inorg. Chem.* **2008**, *47*, 2267; h) J.-H. Yum, I. Jung, C. Baik, J. Ko, M. K. Nazeeruddin, M. Grätzel, *Energy Environ. Sci.* **2009**, *2*, 100; i) Z. Jin, H. Masuda, N. Yamanaka, M. Minami, T. Nakamura, Y. Nishikitani, *J. Phys. Chem. C* **2009**, *113*, 2618; j) C.-Y. Chen, M. Wang, J.-Y. Li, N. Pootrakulchote, L. Alibabaei, C.-H. Ngoc-Le, J.-D. Decoppet, J.-H. Tsai, C. Grätzel, C.-G. Wu, S. M. Zakeeruddin, M. Grätzel, *ACS Nano* **2009**, *3*, 3103; k) Q. Yu, S. Liu, M. Zhang, N. Cai, Y. Wang, P. Wang, *J. Phys. Chem. C* **2009**, *113*, 14559; l) K. Chen, Y.-H. Hong, Y. Chi, W.-H. Liu, B.-S. Chen, P.-T. Chou, *J. Mater. Chem.* **2009**, *19*, 5329.
- [5] a) M. K. Nazeeruddin, A. Kay, I. Rodicio, R. Humphry-Baker, E. Mueller, P. Liska, N. Vlachopoulos, M. Graetzel, *J. Am. Chem. Soc.* **1993**, *115*, 6382; b) M. Grätzel, *J. Photochem. Photobiol. A* **2004**, *164*, 3.
- [6] a) S. H. Wadman, J. M. Kroon, K. Bakker, R. W. A. Havenith, G. P. M. van Klink, G. van Koten, *Organometallics* **2010**, *29*, 1569; b) Y. Sun, A. C. Onicha, M. Myahkostupov, F. N. Castellano, *ACS Appl. Mater. Int.* **2010**, *2*, 2039; c) K.-L. Wu, H.-C. Hsu, K. Chen, Y. Chi, M.-W. Chung, W.-H. Liu, P.-T. Chou,

- Chem. Commun.* **2010**, *46*, 5124; d) K. C. D. Robson, B. D. Koivisto, T. J. Gordon, T. Baumgartner, C. P. Berlinguette, *Inorg. Chem.* **2010**, *49*, 5335; e) H.-J. Park, K. H. Kim, S. Y. Choi, H.-M. Kim, W. I. Lee, Y. K. Kang, Y. K. Chung, *Inorg. Chem.* **2010**, *49*, 7340; f) J.-J. Kim, K. Lim, H. Choi, S. Fan, M.-S. Kang, G. Gao, H. S. Kang, J. Ko, *Inorg. Chem.* **2010**, *49*, 8351; g) X. Lv, F. Wang, Y. Li, *ACS Appl. Mater. Int.* **2010**, *2*, 1980.
- [7] M. K. Nazeeruddin, P. Pechy, T. Renouard, S. M. Zakeeruddin, R. Humphry-Baker, P. Comte, P. Liska, L. Cevey, E. Costa, V. Shklover, L. Spiccia, G. B. Deacon, C. A. Bignozzi, M. Grätzel, *J. Am. Chem. Soc.* **2001**, *123*, 1613.
- [8] M. K. Nazeeruddin, M. Grätzel, *J. Photochem. Photobiol. A* **2001**, *145*, 79.
- [9] B.-S. Chen, K. Chen, Y.-H. Hong, W.-H. Liu, T.-H. Li, C.-H. Lai, P.-T. Chou, Y. Chi, G.-H. Lee, *Chem. Commun.* **2009**, 5844.
- [10] J. B. Lamture, Z. H. Zhou, A. S. Kumar, T. G. Wensel, *Inorg. Chem.* **1995**, *34*, 864.
- [11] Z.-S. Wang, T. Yamaguchi, H. Sugihara, H. Arakawa, *Langmuir* **2005**, *21*, 4272.
- [12] Y. Chiba, A. Islam, Y. Watanabe, R. Komiya, N. Koide, L. Han, *Jpn. J. Appl. Phys.* **2006**, *45*, L638.
- [13] M. K. Nazeeruddin, R. Humphry-Baker, P. Liska, M. Grätzel, *J. Phys. Chem. B* **2003**, *107*, 8981.
- [14] a) M. Miyashita, K. Sunahara, T. Nishikawa, Y. Uemura, N. Koumura, K. Hara, A. Mori, T. Abe, E. Suzuki, S. Mori, *J. Am. Chem. Soc.* **2008**, *130*, 17874; b) T. Marinado, K. Nonomura, J. Nissfolk, M. K. Karlsson, D. P. Hagberg, L. Sun, S. Mori, A. Hagfeldt, *Langmuir* **2010**, *26*, 2592.
- [15] The dipole sign is defined to have a direction pointing from the negative to the positive charge.
- [16] a) S. S. Rühle, M. Greenshtein, S.-G. Chen, A. Merson, H. Pizem, C. S. Sukenik, D. Cahen, A. Zaban, *J. Phys. Chem. B* **2005**, *109*, 18907; b) Z. Zhang, N. Evans, S. M. Zakeeruddin, R. Humphry-Baker, M. Grätzel, *J. Phys. Chem. C* **2007**, *111*, 398; c) W. H. Howie, F. Claeysens, H. Miura, L. M. Peter, *J. Am. Chem. Soc.* **2008**, *130*, 1367; d) P. Chen, J. H. Yum, F. De Angelis, E. Mosconi, S. Fantacci, S.-J. Moon, R. H. Baker, J. Ko, M. K. Nazeeruddin, M. Grätzel, *Nano Lett.* **2009**, *9*, 2487; e) U. B. Cappel, S. M. Feldt, J. Schoeneboom, A. Hagfeldt, G. Boschloo, *J. Am. Chem. Soc.* **2010**, *132*, 9096; f) Y. Liang, B. Peng, J. Chen, *J. Phys. Chem. C* **2010**, *114*, 10992.